Biochimica et Biophysica Acta, 1024 (1990) 336–344
Elsevier

BBAMEM 74847

Study of the topography of cannabinoids in model membranes using X-ray diffraction

Thomas Mavromoustakos [1], De-Ping Yang [1], Avgui Charalambous [1], Leo G. Herbette [3,4] and Alexandros Makriyannis [1,2,4]

[1] *School of Pharmacy and Institute of Materials Science, University of Connecticut, Storrs, CT,* [2] *Francis Bitter National Magnet Laboratory, Massachusetts Institute of Technology, Cambridge, MA,* [3] *Departments of Radiology, Medicine and Biochemistry and* [4] *Biomolecular Structure Analysis Center, University of Connecticut Health Center, Farmington, CT (U.S.A.)*

(Received 9 February 1990)

Key words: X-ray diffraction; DSC; (−)-Δ^8-Tetrahydrocannabinol; (−)-5′-Iodo-Δ^8-tetrahydrocannabinol; Drug–membrane interaction

Small-angle X-ray diffraction was used to determine the topography of (−)-Δ^8-tetrahydrocannabinol in partially hydrated dimyristoylphosphatidylcholine bilayers. Electron density profiles of lipid bilayers in the presence and absence of the cannabinoid were calculated using Fourier transform. Step-function equivalent profiles were then constructed to obtain the absolute electron density scale. We have compared the electron density profiles of the above preparations to determine the location of the drug molecule in the bilayer. By using (−)-5′-iodo-Δ^8-tetrahydrocannabinol in parallel experiments, we were also able to locate the iodine atom in the bilayer and deduce the conformation of the cannabinoid side alkyl chain. All comparisons were made between different preparations having the same mesomorphic form and total period repeat distance. To achieve this, we have carried out X-ray diffraction experiments at various temperatures to cover the different mesomorphic phases and combined our data with the corresponding results from differential scanning calorimetry. Based on the results of this work and previous data on the orientation of the cannabinoid in model membranes, we concluded that the phenolic hydroxy group of the drug molecule exists near the carbonyl groups of DMPC and that the average position of the iodine atom is approx. 5.5 Å from the center (terminal methyl region) of the DMPC bilayer. This requires the cannabinoid side-chain to assume an orientation parallel to the bilayer chains.

Introduction

Many pharmacological actions of cannabinoids are related to their known effects on biological membranes [1–3]. Their molecular mechanism of action, however, is still unknown. In our previous work, we have provided evidence that the geometry of these molecules as well as their amphipathic character are among the principal factors which determine their biological effects [4,5]. This evidence, coupled with other data reported by Bruggemann and Melchior [6], supports a molecular model in which cannabinoids localize near the membrane hydrocarbon-core/water interface, and that the phenolic hydroxy group serves as an anchor for the drug molecule in this region of the bilayer.

In the present work, we have used small-angle X-ray diffraction techniques to study the location of a biologically active cannabinoid in a partially hydrated model membrane and obtained direct evidence on the topography of the drug in the bilayer. Partial hydration provides the sample with some order by packing the lipid bilayer into a stack of lamellae which gives coherent Bragg-like scattering at reasonable resolution. Various diffraction orders are then observed and the entire diffraction pattern can be analyzed to obtain the total period repeat distance (*d*-spacing) as well as the electron density profile.

The method is based on comparing the electron density profiles from membrane preparations without and with cannabinoids. Any observed differences can then provide information on the location of the drugs in

Abbreviations: DMPC, dimyristoylphosphatidylcholine; Δ^8-THC, (−)-Δ^8-tetrahydrocannabinol; 5′-I-Δ^8-THC, (−)-5′-iodo-Δ^8-tetrahydrocannabinol; DSC, differential scanning calorimetry; RH, relative humidity.

Correspondence: A. Makriyannis, School of Pharmacy and Institute of Materials Science, University of Connecticut, Storrs, CT 06269, U.S.A.

the bilayer as well as on the perturbations which these molecules can induce on the bilayer structure.

Cannabinoids are known to broaden the main phase transition of lipid bilayers and lower the transition temperature [5,6]. Therefore, it is possible that at the same temperature, the different membrane preparations may exist in different mesomorphic states (gel or liquid crystalline). Also, the preparations may exist in the same phase but may differ in their conformational properties; for example, they may have different ratios of *gauche : trans* conformers in the methylene segments of the bilayer chains. Consequently, any observed differences in the electron density profiles of two membrane preparations may be due to (a) electron density contribution by the drug molecule; (b) differences in the phase properties of the bilayer preparations; or (c) some combination of these two. In order to differentiate between these two effects, it became necessary to study the thermotropic properties of our membrane preparations by carrying out X-ray diffraction experiments at different temperatures and comparing the results with the phase profiles obtained from differential scanning calorimetric (DSC) data using identical membrane preparations. We were thus able to compare preparations having the same *d*-spacing and mesomorphic phase and attribute the observed differences in the electron density profiles between preparations solely to the presence of the drug in the bilayer. The electron density difference between the DMPC + Δ^8-THC and DMPC preparations gave us information on the location of the tricyclic cannabinoid component in the bilayer. Furthermore, by comparing the Δ^8-THC containing preparation with one in which Δ^8-THC was labelled with an iodine atom at the terminal chain segment, we were able to obtain information on the orientation and conformation of the cannabinoid five-carbon chain.

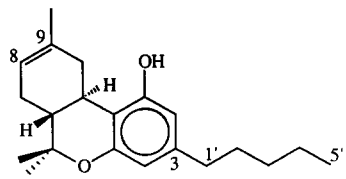

(-)-Δ^8-tetrahydrocannabinol

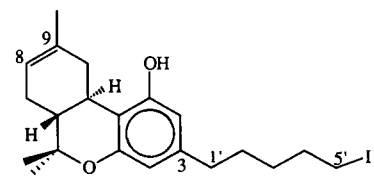

(-)-5'-iodo-Δ^8-tetrahydrocannabinol

Fig. 1. (−)-Δ^8-THC and (−)-5′-I-Δ^8-THC.

Materials and Methods

Materials

(−)-Δ^8-Tetrahydrocannabinol (Δ^8-THC) and (−)-5′-iodo-Δ^8-tetrahydrocannabinol (5′-I-Δ^8-THC) (Fig. 1) were synthesized in our laboratories using methods reported elsewhere [7,8]. Dimyristoylphosphatidylcholine (DMPC) was obtained from Avanti Polar Lipids, Birmingham, AL.

Membrane sample preparation

We have used identical partially hydrated membrane preparations for both the X-ray diffraction and DSC experiments. DMPC (1 mg for X-ray diffraction or 7 mg for DSC) alone or with the appropriate amount of Δ^8-THC and 5′-I-Δ^8-THC were dissolved in chloroform (99 + % pure, Aldrich, Milwaukee, WI). The solvent was then removed using an O_2-free N_2 stream and the samples were dried under vacuum for 6 h. After adding distilled water, each sample was vortexed and sonicated in a water bath (50 °C) for 15 min until the suspension was translucent. For the X-ray diffraction experiments, the preparations were deposited on an aluminum foil, dried at 35 °C and mounted on a curved glass holder. For the DSC experiments, the vesicles were deposited on a glass surface, dried at 35 °C and scraped into stainless-steel DSC pans (0.25 cm height × 0.5 cm diameter). Prior to the experiments, X-ray diffraction samples and DSC samples were suspended in closed vials (5 cm height × 3 cm diameter) with regulated relative humidities (RH) using appropriate saturated salt solutions for 24 h and 48 h, respectively. This produces partially hydrated multilamellar vesicles. The salts (Sigma, St. Louis, MO) for the various relative humidities were LiCl for RH 13%, $NaNO_2$ for RH 66% and K_2SO_4 for RH 98%. For the X-ray experiments, the preparations were transferred into RH-regulated containers (5 cm height × 3 cm diameter) 3–5 h before the experiments. To keep the partial hydration of the DSC samples constant, the samples were sealed hermetically in stainless steel capsules. We found that partially hydrated samples prepared in this manner gave identical thermograms when tested repeatedly over a 7-day period, indicating that there was no change in the water content of the sample.

Differential scanning calorimetry

Thermograms were obtained on a Perkin-Elmer DSC-7 instrument. Prior to scanning, samples were held above their transition temperature for 1–2 min to ensure complete equilibration. All samples were scanned at least twice until identical thermograms were obtained. Heating and cooling scans gave similar results. Only beyond 5.0 K/min did the scanning rate affect the thermograms by slightly broadening the breath of the phase transition and shifting the main phase transition. We thus used a scanning rate of 1.5 K/min. The temperature scale of the calorimeter was calibrated using

both fully hydrated DPPC and indium as standard samples. We also examined the effect of the equilibration time. Identical thermograms were obtained if more than 48 h equilibration time was allowed.

X-ray diffraction

X-ray diffraction experiments were carried out with an Elliott GX18 generator (Marconi Avionics), equipped with a camera utilizing a single vertical Franks' mirror [9]. Small angle X-ray diffraction patterns were collected using a Braun position-sensitive proportional counting (PSPC) gas flow detector (Innovative Technology, South Hamilton, MA). During the experiment, we used a helium path for a specimen-to-detector distance of 130 mm and collected the diffraction data with digital accumulations of $1 \cdot 10^6$ to $2 \cdot 10^6$ counts to improve the signal-to-noise ratio. Data was transferred to a VAX computer system and the intensities were integrated directly from the computer plots by calculating the area under the diffraction peaks. Wide-angle patterns were recorded on films with a specimen-to-film distance of 35 mm.

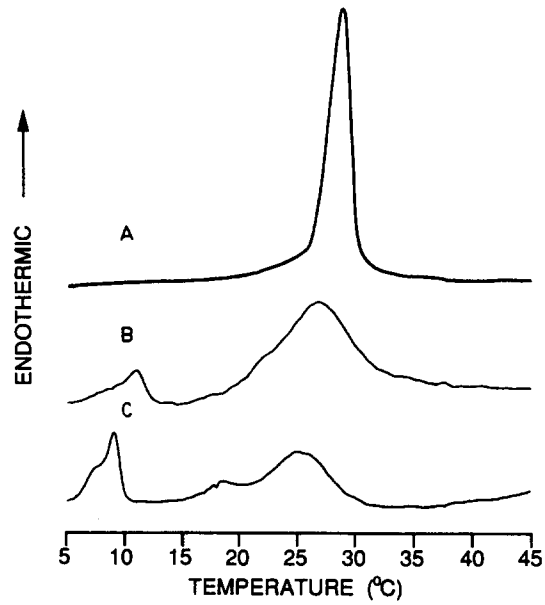

Fig. 2. Thermograms of partially hydrated bilayers at RH 98% of (A) DMPC, (B) DMPC + Δ^8-THC and (C) DMPC + 5′-I-Δ^8-THC. The lipid-to-drug molar ratio is 85 : 15, or $x = 0.15$.

Results and Analysis

Differential scanning calorimetry

In order to analyze quantitatively our small-angle X-ray diffraction data we needed information on the mesomorphic properties of our partially hydrated sample preparations. For this purpose, we carried out parallel DSC experiments using DMPC preparations equilibrated at three relative humidities, RH 13%, RH 66% and RH 98%, within temperature ranges covering the mesomorphic phases of interest. The scanning temperature range depended on the amount of hydration of the sample since it is known that for synthetic phospholipids a decrease in hydration increases the main phase-transition temperature, T_c [10].

Representative thermograms from DMPC preparations equilibrated at RH 98% and from similar preparations containing Δ^8-THC or 5′-I-Δ^8-THC (molar ratio 85 : 15, or $x = 0.15$) are shown in Fig. 2. The partially hydrated DMPC bilayers (A) showed a relatively sharp phase transition at 29 °C, approx. 5 K higher than that observed with the fully hydrated preparation. However, the pretransition which always appears in thermograms of fully hydrated saturated phosphatidylcholines was absent. A similar observation was made by Janiak et al. with sample preparations having water concentrations of less than 20% (w/w) [11]. The presence of the cannabinoid broadened significantly the main phase transition. Two peaks are prominent in the thermograms containing either Δ^8-THC (B) or 5′-I-Δ^8-THC (C); a broad main transition peak centered at a temperature 2–3 K below that of the main transition of pure DMPC and a relatively sharp peak centered at approx. 15–17 K prior to the main phase transition.

X-ray diffraction

We have carried out small-angle X-ray experiments using DMPC bilayers without and with Δ^8-THC or 5′-I-Δ^8-THC ($x = 0.15$) equilibrated at three relative humidities (RH 13%, RH 66% and RH 98%) within a temperature range covering the main phase transition as observed in the thermograms. At temperatures below the phase transition, diffraction patterns with up to eight orders ($h = 8$) were observed and recorded with digital resolution of 30 channels/mm. At temperatures above the phase transition four diffraction orders were collected. Since sample preparation conditions were critical for gaining accurate and reliable results, experiments were repeated six times. The results reported here are from one of these experiments and are consistent with the other data.

In order to obtain information on any changes in the chain packing when a cannabinoid is incorporated into the DMPC bilayer, we also carried out wide-angle diffraction experiments for the three preparations equilibrated at RH 98% at 35 °C. The results showed a diffused band of equatorial diffraction corresponding to a two-dimensional chain-packing lattice of 4.74 ± 0.06 Å, 4.68 ± 0.06 Å and 4.74 ± 0.06 Å for DMPC, DMPC + Δ^8-THC and DMPC + 5′-I-Δ^8-THC, respectively. It thus appears that in concentrations up to at least $x = 0.15$, cannabinoids produce no significant expansion in the chain-packing lattice of the DMPC bilayer preparations we used in our analysis.

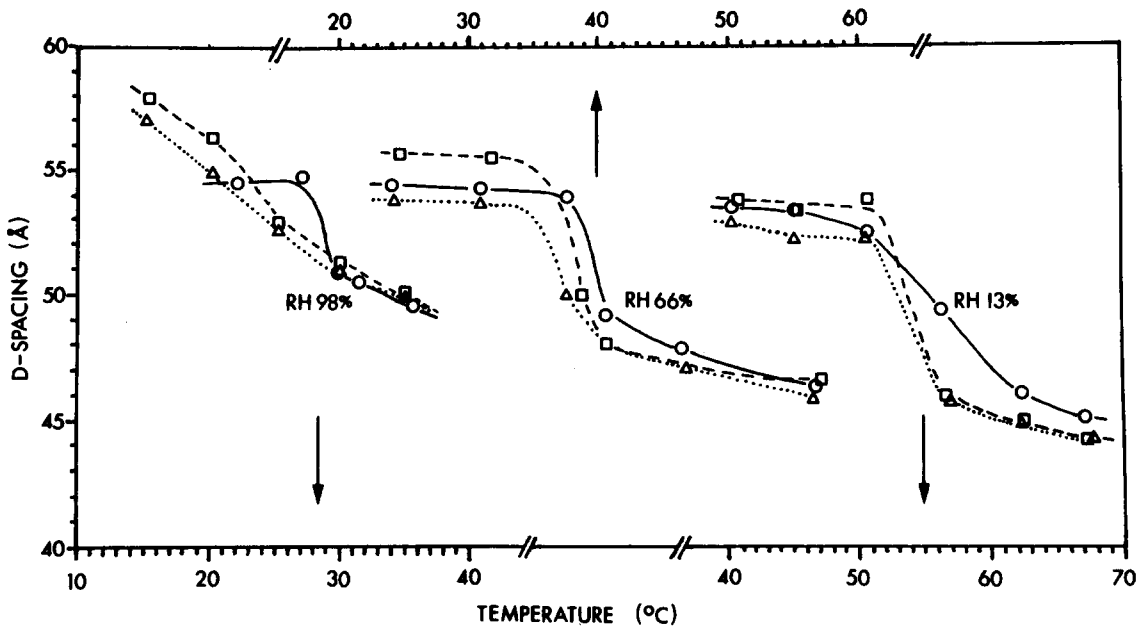

Fig. 3. *D*-Spacing versus temperature for bilayer preparations of DMPC (○———○), DMPC + Δ^8-THC ($x = 0.15$, △·····△), and DMPC + 5′-I-Δ^8-THC ($x = 0.15$, □-----□) equilibrated at RH 98% (left), RH 66% (middle) and RH 13% (right). Note that the left and right curves use the bottom temperature scales while the middle curves use the top temperature scale.

The analysis of the small angle diffraction results involved calculating the total period repeat distance (*d*-spacing) using Bragg's Law, determining the signs of the structure factors using the bilayer swelling approach, and obtaining the electron density profile using a Fourier transform algorithm. The electron density profiles were then placed on the absolute scale using the step-function model method. Information on the location of the drug in the bilayer was obtained by comparing the electron density profiles of the DMPC preparations without and with the cannabinoids.

Temperature and humidity dependences of d-spacing

The small angle diffraction peaks in each diffraction pattern were analyzed to give the *d*-spacing. Fig. 3 shows the *d*-spacing values as a function of temperature for each of the three preparations equilibrated at three relative humidities. As can be seen, all the transitions from the gel to the liquid crystalline phase correspond to a decrease in the *d*-spacing. As is characteristic for such systems, the more ordered the bilayer is, the sharper the transition, corresponding to a steeper decrease in *d*-spacing. The pure DMPC preparations showed the following features: (1) The *d*-spacing remained constant below the main phase transition, up to temperatures of 28, 38 and 45 °C for RH 98%, RH 66% and RH 13%, respectively. (2) A decrease in the hydration of the bilayer is accompanied by increasingly broader main transitions and higher transition temperatures. (3) Above the main phase transition, the *d*-spacing values decreased gradually and continuously. The principal difference in the phase properties of the DMPC bilayers produced by the cannabinoid is that these preparations now had a sharp main phase transition at low relative humidity which became progressively broader with increasing hydration, a trend opposite to that observed in pure DMPC.

Measurement of the *d*-spacings of the different DMPC preparations as a function of temperature and humidity allowed us to follow the phase changes and to choose preparations having similar *d*-spacings when comparing electron density profiles.

Determination of the structure factor signs

We have utilized the *d*-spacing values for temperatures above the phase transition as a function of water content to determine the structure factor signs, which were not readily obtainable from a single diffraction experiment. With all the preparations in the liquid crystalline phase, the *d*-spacing increased with increasing relative humidity. The corresponding diffraction intensities in this 'swelling experiment' were then used to determine the signs of the structure factors [12]. This approach assumes that the introduction of water between the DMPC bilayers does not modify their structure and maintains their integrity. Thus, the water serves only to move the bilayers further apart and increase the *d*-spacing. The structure of the membrane bilayer is considered to be centrosymmetric and each diffraction amplitude (square-root of intensity) has a phase angle of either 0 or π and can be positive or negative. The signs can then be deduced by observing the behavior of the amplitude versus the reciprocal *d*-spacing at or near the zeros of intensity [13].

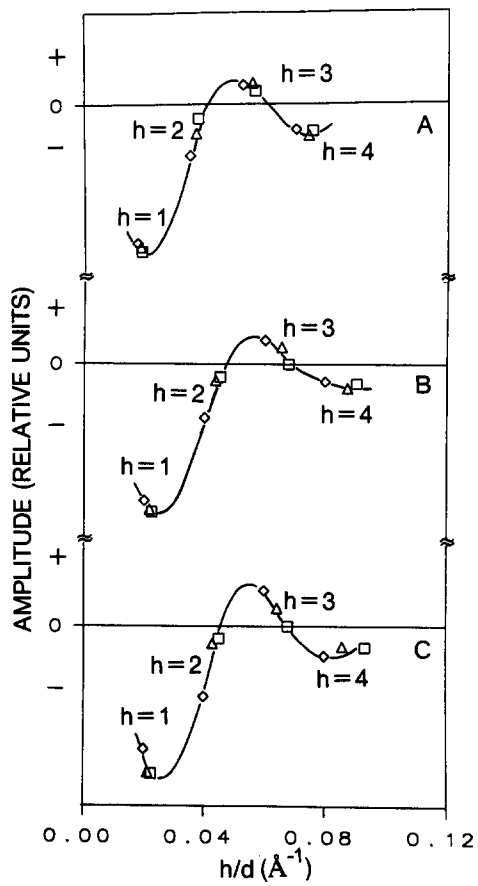

Fig. 4. Diffraction amplitude vs. h/d for DMPC (A), DMPC + Δ^8-THC (B) and DMPC + 5′-I-Δ^8-THC (C) equilibrated at RH 98% (◇), RH 66% (△) and RH 13% (□).

Fig. 4 shows the diffraction amplitudes for DMPC preparations with and without cannabinoid as a function of the reciprocal d-spacing for three relative humidities (RH 13%, RH 66% and RH 98%). Data points for DMPC alone (curve A) and those containing a cannabinoid (curves B and C) fall on similar smooth curves which provide reliable evidence that the DMPC bilayers without and with cannabinoid have same signs for the structure factors and that no structural change occurred during the bilayer expansion. The signs were found to be −, −, + and − for the structure factors corresponding to the 1st, 2nd, 3rd and 4th orders, respectively.

Electron density profile calculation

We calculated electron density profiles for the centrosymmetric bilayers from the integrated intensity values for the various orders of the diffraction pattern and the structure factors just determined, using a Fourier transform algorithm described by Franks and Levine [14]. In Fig. 5, we present a typical electron density profile in the dimension z across the DMPC bilayers equilibrated at RH 98% at 22° C. A molecular graphical representation of the DMPC bilayer shown above the electron density profile serves to correlate the molecular features of the bilayer with its corresponding electron density values. As can be seen, maximum electron density corresponds to the phospholipid head group while the terminal methyl group region has the lowest density. The electron density profiles described above are on a relative scale, since they were obtained from the relative intensities of the various diffraction orders. In order to complete the analysis quantitatively, it was necessary to obtain the absolute scale for the electron density profiles.

Absolute electron density scale determination

We have followed an approach in which a step-function equivalent profile was calculated for the DMPC preparation and placed on the absolute electron density scale. We were then able to assign absolute values to the corresponding experimentally obtained electron density profile by superimposing onto it the above-developed step-function.

This one-dimensional electron density step-function model was first introduced as an alternative to the Fourier transform analysis of low-angle, X-ray diffraction data [15]. The method involves proposing a step-function model for the electron density across the bilayer and testing its correctness by comparing the ratios of the calculated and observed amplitudes of the diffraction orders. The step-function approach was further developed and used successfully to determine the bilayer hydrocarbon thickness through analysis of neu-

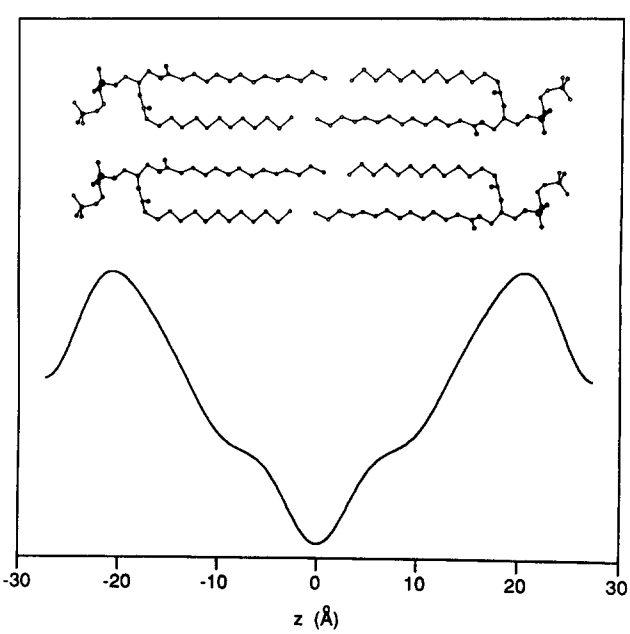

Fig. 5. Electron density profiles obtained by Fourier transformation of the small angle diffraction intensities for DMPC at 22° C equilibrated at RH 98%. A molecular graphic representation of a DMPC bilayer above the electron density profile shows the space correlation in the dimension across the bilayer.

tron diffraction data and the mathematical details of the procedure have been described [16]. Although the step-function model itself is still on a relative electron density scale, it allows us to assign the absolute values to those regions where the average electron densities have been determined by other means. Additionally, this model provides the structure factor signs, which can be compared with the signs obtained from the swelling experiment.

Our DMPC preparation at 35 °C gave a four-order X-ray diffraction pattern. For our step-function analysis, we constructed a four-step model representing four corresponding regions of the bilayer, namely, the terminal methyl, fatty acyl methylene, head group and water regions. This model involves eight parameters, i.e., four electron density levels and four locations of the boundaries between the adjacent regions. Of the four relative electron density levels, only two are independent. On the other hand, the experimental value for the *d*-spacing allows us to reduce the number of boundary parameters from four to three. The model thus can be represented by a total of five independent parameters. Using a reverse Fourier transformation, the step-function can be converted into a set of simulated diffraction amplitudes with their signs. The five parameters can then be adjusted iteratively so that the first four simulated amplitudes match the values of the experimental amplitudes and the signs agree with the results obtained from the swelling approach. For the DMPC preparation at 35 °C equilibrated at RH 98% and with a *d*-spacing of 50.4 Å, best fit was obtained with boundaries between the four regions equal to 5.7 Å, 13.5 Å and 20.8 Å, starting from the center of the bilayer. The corresponding relative electron density levels in the four regions were found to be 0.00, 0.40, 1.00 and 0.82.

To calculate the corresponding absolute electron densities, we made use of values previously determined for similar systems. The DPPC bilayer was reported to have absolute electron density values of 0.194, 0.260, 0.430 and 0.334, respectively, for the terminal methyl, fatty acyl methylene, head group and water regions [17]. Since DMPC is structurally identical to DPPC except for having the acyl chains shorter by two methylene groups, we adopted the head group and terminal methyl DPPC absolute values for the step-function of our DMPC bilayer. In this manner, we were able to convert the previously determined relative electron density levels for DMPC to the corresponding absolute values. These were found to be 0.194, 0.288, 0.430 and 0.388 electron per $Å^3$, as shown in the graphic representation of the step-function (Fig. 6).

The differences between diffraction intensities simulated from the step-function and experimental ones were within 1%. Also, the signs of the structure factors calculated from the step-function model were identical to those obtained in the swelling experiment. The average electron densities in the other two regions (methylene and water) were in general agreement with the accepted values in the same regions. Furthermore, this absolute scale for the electron density profile which we determined for DMPC is consistent with the absolute scale for a similar system involving DMPC and cholesterol [18]. This assured us that we had obtained a reasonable model.

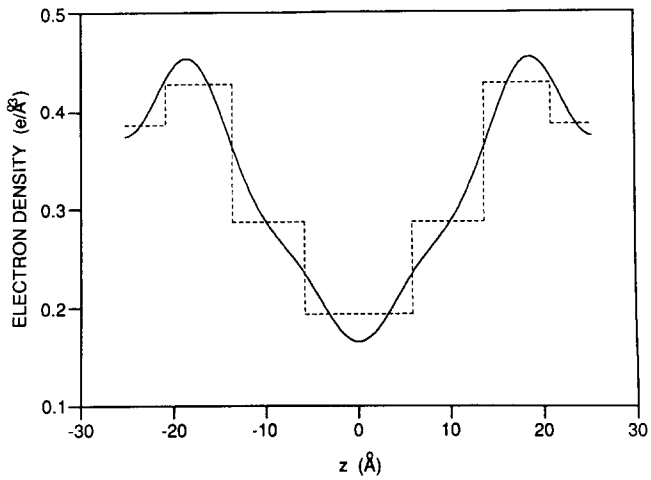

Fig. 6. Step-function equivalent profile (dashed line) and the corresponding continuous electron density profile (solid line) on the absolute scale for a DMPC bilayer at 35 °C equilibrated at RH 98%. The spacing of the scale is absolute but its zero may not be. The terminal methyl and head group regions were used to assign the absolute values of the density based on previously reported results.

The last step in the determination of the absolute scale for our electron density profile involved superimposing the above calculated step-function onto the corresponding continuous profile obtained by Fourier synthesis of the experimental data. For this superposition, we have allowed the step-function electron density levels in the head group and the terminal methyl regions equal to the average electron density values of the respective continuous profile. This was achieved by calculating simultaneously a multiplicative factor and an additive constant that brought the continuous profile to the absolute scale, as shown by the solid line in Fig. 6.

Location of cannabinoid molecule in the bilayer

In order to find the position of the cannabinoid molecule in the bilayer, we have compared the electron density profiles of DMPC alone, DMPC + Δ^8-THC and DMPC + 5′-I-Δ^8-THC preparations. The most prominent difference was observed at RH 98% at temperatures above the phase transition. At 35 °C, the three preparations had identical *d*-spacing. Therefore, they were in the same mesomorphic state and had the same *gauche : trans* conformer ratio, providing the best condition for comparison. In this manner, we ensured that any difference between the profiles was solely due to the presence of the cannabinoid.

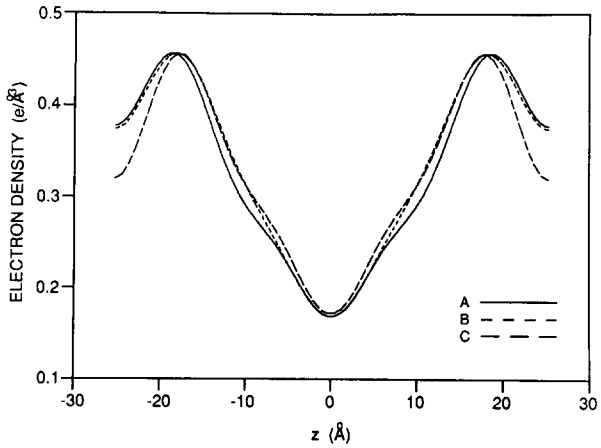

Fig. 7. Comparison of electron density profiles of DMPC (A, solid line), DMPC + Δ^8-THC (B, short dashed line) and DMPC + 5′-I-Δ^8-THC (C, long dashed line) at 35 °C equilibrated at RH 98%.

Our earlier experimental data had placed Δ^8-THC somewhere near the bilayer interface [19]. We can thus argue that this molecule when incorporated in the membrane does not make a significant electron density contribution either to the phospholipid head group or to the terminal methyl groups of the fatty acyl chains. Therefore, for our comparisons, we have assumed that the DMPC and DMPC + Δ^8-THC preparations had identical electron densities at the level of the head groups and terminal methyl groups. On this basis, we have superimposed the profiles of the above two preparations as shown in Fig. 7 (A and B) and focused our comparisons on the electron density differences at the interface and fatty acyl chain regions of the bilayer corresponding to $|z| \leq 18$ Å. The difference of the two profiles is shown in Fig. 8 (B − A) and exhibits an increase in electron density for the DMPC + Δ^8-THC preparation in a region centered at $z = 12.2$ Å. This electron density difference corresponds to 0.2060 e/Å^2 as calculated by integration from $z = 0$ to $z = 18$ Å.

When the electron density profile from DMPC + 5′-I-Δ^8-THC was compared to that from DMPC + Δ^8-THC, an increase was observed in the region corresponding to the inner chain segments, presumably due to a contribution from the iodine atom on 5′-I-Δ^8-THC. We have calculated the expected increase in integrated electron density between the two preparations using the following rationale: When a methyl hydrogen in Δ^8-THC is substituted with an iodine in 5′-I-Δ^8-THC, there is an increase in the total number of electrons from 172 (Δ^8-THC) to 224 (5′-I-Δ^8-THC). This increase should correspond to a change of absolute integrated difference from 0.2060 e/Å^2 (between DMPC + Δ^8-THC and DMPC) to 0.2682 e/Å^2 (between DMPC + 5′-I-Δ^8-THC and DMPC).

Using the above computed absolute electron density difference, our next task was to superimpose the electron density data from the DMPC + 5′-I-Δ^8-THC preparation onto the control DMPC. For this superposition, we first used identical absolute electron densities for the head group and methyl group regions, as we did with the corresponding Δ^8-THC preparation, assuming that the entire contribution of the iodo group was in the acyl methylene region. However, this approach could not account for the total calculated difference of 0.2682 e/Å^2. A superposition of the experimentally obtained electron density profiles which fully accounts for the calculated electron density difference was accomplished by placing the trough of the DMPC + 5′-I-Δ^8-THC profile at 0.003 e/Å^3 above that of DMPC while maintaining the same electron density at the head group region as shown in Fig. 7 (A and C). This approach to normalize the two profiles can be justified by arguing that, because of its distal position in the molecule, the iodo group has some contribution in the inner region of the bilayer. Also, this effect is congruent with the observation that the difference in the experimentally obtained electron density profiles between the two drug-containing preparations extended into the center of the bilayer. At the same time we do not expect the iodine atom to significantly affect the electron density in the head group region.

The profile difference between the curves C and A is plotted in Fig. 8 (C − A) and shows a peak extending from about 18 Å almost through the center of the bilayer. Also shown in Fig. 8 is the difference between

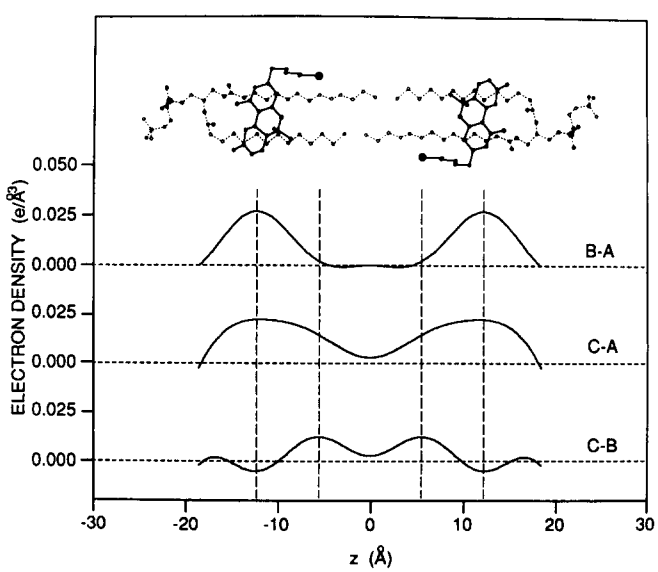

Fig. 8. Electron density profile differences inside the bilayer: Curve B − A is the difference between profiles of DMPC + Δ^8-THC and DMPC, curve C − A is the difference between those of DMPC + 5′-I-Δ^8-THC and DMPC, and curve C − B is the difference between those of DMPC + 5′-I-Δ^8-THC and DMPC + Δ^8-THC. The outer pair of the vertical dashed lines indicates the peaks in curve B − A and the inner pair indicates the peaks in C − B. They represent the positions of the center of Δ^8-THC and the iodine atom of 5′-I-Δ^8-THC in the bilayer, respectively, as shown by the graphic representations of the molecules above.

profiles of the two drug-containing preparations (C – B) where a peak centered at 5.5 Å represents an increase in electron density in that region presumably due to the iodine atom. Graphic representations of DMPC and 5′-I-Δ^8-THC molecules are also shown to scale in Fig. 8 to serve as a visual aid for the locations of the drug and the iodine atom.

Discussion and Conclusions

In this work, we have studied the thermal properties of partially hydrated DMPC bilayers with and without cannabinoids to obtain the appropriate temperature ranges for the small-angle X-ray diffraction experiments. Temperature and humidity dependences of the *d*-spacing within the same temperature ranges were in excellent agreement with the DSC results. The gradual and continuous decrease of *d*-spacing at temperatures above the phase transition can be accounted for by an increase in the *gauche : trans* conformer ratio with higher temperatures. The observations paralleled the changes in the quadrupolar splittings ($\Delta\nu_Q$) observed in solid state ^{2}H-NMR spectra in the liquid crystalline phase, using ^{2}H-labeled phospholipids [20].

Our bilayer preparations were equilibrated at three different relative humidities and the *d*-spacing data were analyzed to provide the structure factor signs, which were in agreement with the results previously reported for DMPC [21]. Our results from the drug-containing preparations showed that the presence of a cannabinoid changed only the amplitudes of the structure factors but not their signs. This fact implied that the drug molecules do not induce significant structural changes in the bilayer. This allowed us to calculate the electron density profiles using the same set of signs for all three bilayer preparations and to compare them.

The construction of a step-function equivalent profile for DMPC was used as method for obtaining the absolute scale for the electron density profile. By comparing the electron density profiles of three DMPC preparations which had identical phase and conformational properties, we were able to obtain topographical information on two molecular components of Δ^8-THC. First, a comparison between DMPC and DMPC + Δ^8-THC identified, within the bilayer, the location of the principal THC component, namely, the tricyclic ring structure. Subsequently, we compared the DMPC + Δ^8-THC and DMPC + 5′-I-Δ^8-THC preparations to gain information on the location of the iodo group in the terminal chain segment of the cannabinoid. This second comparison required appropriate normalization of the electron density profiles to account for the expected increase in electron density due to the presence of the iodo group. This normalization resulted in a slight increase in electron density at the profile trough for the preparation containing the iodinated THC. Such an increase can be explained by invoking some contribution of the iodo group in the terminal methyl region of the bilayer.

By plotting the difference between electron density profiles, we can obtain an improved representation of the site of increased electron density in the bilayer. Although the resolution is about 6 Å in the electron density profiles transformed from four orders of diffraction, the maximum in the profile difference indicates the most probable location of the center of the drug in the bilayer. Our data from the DMPC + Δ^8-THC preparation equilibrated at RH 98% at 35 °C show that the center of the tricyclic ring system of Δ^8-THC resides approx. 12 Å from the center of the bilayer. On the other hand, the comparison between the electron density profiles of DMPC + 5′-I-Δ^8-THC and DMPC + Δ^8-THC placed the iodine atom approx. 5.5 Å from the center of the bilayer.

Earlier work from our laboratory using solid-state ^{2}H-NMR has shown that Δ^8-THC orients with the long axis of its tricyclic system perpendicular to the bilayer chains [22]. Combined with our present X-ray diffraction results, such an orientation would place the phenolic hydroxy group of Δ^8-THC near one of the DMPC carbonyl groups, preferably the one of the *sn*-1 chain, allowing for a possible hydrogen bond formation. The calculated location of the iodo group of 5′-I-Δ^8-THC requires the cannabinoid five-membered chain to orient towards the center of the bilayer and parallel to the lipid chains. This cannabinoid chain orientation can be obtained by invoking one *gauche* methylene conformer around the $C_{1'}$–$C_{2'}$ bond followed by two *trans* conformers around $C_{2'}$–$C_{3'}$ and $C_{3'}$–$C_{4'}$ bonds.

Existing evidence indicates that cannabinoids induce their biological effects, at least in part, by interacting with membrane lipids. Our X-ray data show that a biologically active cannabinoid with a free phenolic hydroxyl resides near the bilayer interface. We have also shown that such cannabinoids can very effectively perturb the membrane bilayer, unlike the inactive *O*-methyl analogs which apparently reside near the center of the bilayer and produce no significant perturbations. It is, therefore, tempting to speculate that the location of the drug in the bilayer plays an important role in its ability to perturb biological membranes.

Recently, some of the cannabinoid functions have been attributed to their interactions with specific sites on membrane associated proteins [23]. It can be argued that because of their lipophilic properties cannabinoids diffuse through the membrane lipid bilayer to reach these protein sites. Consequently, the location of the drug in the bilayer may determine its ability to reach these sites in the proper orientation so that it can interact productively with them. According to this hypothesis, the X-ray diffraction data described here may

imply that the cannabinoid binding sites are also located near the membrane interface where they are accessible to the drug.

Acknowledgments

This work was supported by grants from the National Institute on Drug Abuse (DA-3801) and the University of Connecticut Research Foundation (UCRF-35491). The X-ray diffraction experiments of this work were carried out in the Biomolecular Structure Analysis Center at the University of Connecticut Health Center. The Structure Center acknowledges support from the State of Connecticut Department of Higher Education's High Technology Program. We would like to thank Professor David Rhodes, Mark Trumbore, Dr. Preston Mason and Steve Blechner for their help in the experimental part of this work and Xiangqun Xie for obtaining the graphical representations. We also thank the staff of the Structure Center for their dedication in keeping the facilities in optimal running condition. L.G.H. is an Established Investigator of the American Heart Association.

References

1 Martin, B.R. (1986) Pharmacol. Rev. 38, 45–74.
2 Hillard, C.J., Bloom, A.S. and Houslay, M.D. (1986) Biochem. Pharmacol. 35, 2797–2803.
3 Hillard, C.J., Harris, R.A. and Bloom, A.S. (1985) J. Pharmacol. Exp. Ther. 232, 579–588.
4 Makriyannis, A. (1988) in NMR Spectroscopy in Drug Research, Proceedings of the Alfred Benzon Symposium 26 (Jaroszewski, J.W., Schaumburg, K. and Kofod, H., eds.), pp. 437–451, Munksgaard, Copenhagen.
5 Van der Schyf, C.J., Mavromoustakos, T. and Makriyannis, A. (1988) Life Sci. 42, 2231–2239.
6 Bruggemann, E.P. and Melchior, D.L. (1983) J. Biol. Chem. 258, 8298–8303.
7 Banijamali, A., Abou-Taleb, N., Van der Schyf, C.J., Charalambous, A. and Makriyannis, A. (1988) J. Label. Comp. Radiopharm. 25, 73–82.
8 Pitt, C.G., Hobbs, D.T., Schran, H.C., Twine, C.E., Jr. and Williams, D.L. (1975) J. Label. Comp. 11(4), 551–575.
9 Franks, A. (1977) Sci. Prog., Oxf. 64, 371–422.
10 Chapman, D. (1977) in Biological Membranes (Chapman, D. and Wallach, D.F.H., eds.), pp. 91–144, Academic Press, London.
11 Janiak, M.J., Small, D.M. and Shipley, G.G. (1976) Biochemistry 15, 4575–4580.
12 Moody, M.F. (1963) Science 142, 1173–1174.
13 Finean, J.B. and Burge, R.E. (1963) J. Mol. Biol. 7, 672–682.
14 Franks, N.P. and Levine, Y.K. (1981) in Membrane Spectroscopy (Grell, E., ed.), pp. 437–487, Springer, New York.
15 Worthington, C.R. (1969) Biophys. J. 9, 222–234.
16 King, G.I. and White, S.H. (1986) Biophys. J. 49, 1047–1054.
17 Trumbore, M., Chester, D.W., Moring, J., Rhodes, D. and Herbette, L.G. (1988) Biophys. J. 54, 535–543.
18 Franks, N.P., Arunachalam, T. and Caspi, E. (1978) Nature 276, 530–532.
19 Makriyannis, A. and Yang, D.P. (1989) in Molecular and Cellular Mechanisms of Antiarrhythmic Agents (Hondeghem, L., ed.), pp. 293–305, Futura, Mount Kisco.
20 Makriyannis, A., Banijamali, A. and Van der Schyf, C.J. (1987) in Structure Activity Relationships of Cannabinoids (Rapaka, R.S. and Makriyannis, A., eds.), pp. 123–133, NIDA Research Monograph 79.
21 Janiak, M.J., Small, D.M. and Shipley, G.G. (1979) J. Biol. Chem. 254, 6068–6078.
22 Makriyannis, A., Banijamali, A., Jarrell, H.C. and Yang, D.P. (1989) Biochim. Biophys. Acta 986, 141–145.
23 Devane, W.A., Dysarz, F.A., III, Johnson, M.S., Melvin, L.S. and Howlett, A.C. (1988) Mol. Pharmacol. 34, 605–613.